

Impacts of the G145R Mutation on the Structure and Immunogenic Activity of the Hepatitis B Surface Antigen: A Computational Analysis

Reza Rezaee,¹ Mansour Poorebrahim,² Saeideh Najafi,³ Solmaz Sadeghi,² Alieh Pourdast,⁴ Seyed Moayed Alavian,^{5,6} Seyed Ehsan Alavian,^{5,6} and Vahdat Poortahmasebi^{7,*}

¹Ministry of Health and Medical Education, Deputy of Curative Affairs, Budget Administration, Tehran, IR Iran

²Department of Medical Biotechnology, School of Advanced Technologies in Medicine, Tehran University of Medical Sciences, Tehran, IR Iran

³Department of Microbiology, Tonekabon branch, Islamic Azad University, Tonekabon, Mazandaran, IR Iran

⁴Department of Infectious Diseases, Imam Khomeini Hospital Complex, Tehran University of Medical Sciences, Tehran, IR Iran

⁵Middle East Liver Diseases (MELD) Center, Tehran, IR Iran

⁶Baqiyatallah Research Center for Gastroenterology and Liver Diseases, Baqiyatallah University of Medical Sciences, Tehran, IR Iran

⁷Hepatitis B Molecular Laboratory, Department of Virology, School of Public Health, Tehran University of Medical Sciences, Tehran, IR Iran

*Corresponding author: Vahdat Poortahmasebi, Hepatitis B Molecular Laboratory, Department of Virology, School of Public Health, Tehran University of Medical Sciences, P. O. Box: 151556446, Tehran, IR Iran. Tel: +98-2188992660, E-mail: poortahmasebi@razi.tums.ac.ir

Received 2016 May 10; Revised 2016 May 17; Accepted 2016 June 11.

Abstract

Background: Vaccine-escaped hepatitis B virus (HBV) mutations occur within the “a” determinant area, which is located in the major hydrophilic region (MHR) of the hepatitis B surface antigen (HBsAg) protein. It is now well established that the common G145R mutation is highly capable of escaping from HBsAg immune recognition. However, the impacts of this mutation on the structure and immunogenic activity of HBsAg have been poorly investigated.

Objectives: The present study analyzed the effects of the G145R mutation on the structure and immunogenic activity of the HBsAg.

Materials and Methods: Three-dimensional (3D) structure of HBsAg for both the wild-type and G145R mutant were predicted and refined using several web tools. After quantitative evaluations, the effects of the G145R mutation on the secondary and 3D structures of the HBsAg were investigated. In parallel, the immunogenic activity of the wild-type and mutant HBsAg was also analyzed using a ClusPro docking server as well as the IEDB web tool. Further analyses were performed via molecular dynamics (MD) simulations using the GROMACS v5.0.2 simulation package.

Results: The G145R mutation causes a considerable reduction in the immunogenic activity of the HBsAg through a conformational change in the HBsAg antigenic loops. This mutation inserts a new β -strand in the “a” determinant region of the HBsAg, leading to a reduced binding affinity to its monoclonal antibody, MA12. The G145R mutation also increased the compactness and stability of the HBsAg by enhancing the rigidity of the “a” determinant.

Conclusions: These data will be beneficial for designing more advanced antibodies for the recognition of the HBsAg in diagnostics. In addition, the results of this study may assist in the design or development of more effective hepatitis B vaccines.

Keywords: G145R Mutation, HBsAg Mutations, Vaccine Escape Mutations

1. Background

The hepatitis B virus (HBV) is an enveloped virus with an outer diameter of approximately 42 nm contained within a nucleocapsid. Capsids enclose a single copy of the 3.2-kb, partially double-stranded DNA genome, which is covalently linked to the viral polymerase at the 5' end of the full-length minus strand. Coding regions in the HBV genome are organized into four overlapping reading frames (ORFs) designated C (core), P (polymerase), S (surface), and X (a regulatory protein), which are subsequently translated into the corresponding viral proteins (1).

The HBV envelope proteins can be translated from a single ORF: L (large), M (middle), and S (small) or the hepatitis B surface antigen (HBsAg) (1). The HBsAg is composed

of four transmembrane helices that are involved in the integration of protein into the endoplasmic reticulum (ER) membrane. Other regions of the HBsAg are highly coiled, and the coil is responsible for protein's antigenicity (2). There is a major hydrophilic region (MHR) that encompasses amino acid residues 99 and 160, which contains the major epitopes for the induction of a humoral immune response (3, 4). The “a” determinant domain (amino acid positions 121 - 147), which is a highly conserved region of the HBsAg, is located on the exterior surface of the MHR and is involved in the binding of antibodies (anti-HBs) against HBsAg (4, 5). Several HBV mutations within the “a” determinant of the HBsAg have been reported as immune escape mutations, which can potentially be involved in vaccine-induced immunity and diagnostic-escape variants (4). The

commonest type of these mutations, G145R, is created by the substitution of arginine for glycine has been shown to exhibit various degrees of altered binding of HBsAg to antibodies in different commercial assays (6, 7). G145R mutant has been reported in many cases of occult hepatitis B infection (OBI) because it decreases the HBsAg levels (8, 9), often going undetected by routine assays (10) and in patients who suffer from lamivudine-resistant mutants (11). HBV has been classified into eight genotypes (A - H) based on sequence divergence in the genome (12). G145R mutants have mainly been found in genotypes B, C, and D (13). Naturally occurring G145R mutants are often detectable with monoclonal antibody-based assays, albeit at a reduced sensitivity (14).

Previous studies have indicated that the “a” determinant region interacts with the antibodies from patient serum (15) or the mouse monoclonal antibody produced against HBsAg (16). One of the obstacles to detecting a variant critically depends on the choice of the antibody. In contrast, the fundamental difficulty in the *in vitro* characterization of all this variation is the difficulty in the quantitation of the expressed HBsAg in a way that does not depend on its antigenicity. One approach involves the use of an antibody that binds to a common region away from the variant domains being tested, but how can one be sure that the structural conformation is not affected? Moreover, due to a lack of crystallization of wild-type HBsAg molecules and membrane-spanning (17, 18), no template structure exists in the protein data bank (PDB) library for the HBsAg (19).

2. Objectives

The objectives of this *de novo* study were to assess the impact of the G145R mutation on the HBsAg structure at both the two-dimensional (2D) and three-dimensional (3D) levels. We also performed molecular docking studies of the HBsAg-antibody to investigate the antigen-antibody interactions in the G145R mutant compared with the wild-type HBsAg.

3. Materials and Methods

3.1. 2D Analysis and Transmembrane Topology

Predictions regarding the secondary structures of both wild-type (accession numbers: GQ183486) and G145R mutant HBsAg were carried out using three highly accurate secondary structure prediction tools: Jpred 4, PHD, and PSIPRED (20-22). Three different servers were used to elevate the accuracy of the predictions. In parallel, the MEMSAT3 and TMPred web tools (http://embnet.vital-it.ch/software/TMPRED_form.html) were also applied to

predict the orientation and topology of the transmembrane regions of the G145R mutant compared with the wild-type HBsAg (23).

3.2. 3D Analysis and Structural Alignment

Using the amino acid sequence of the HBsAg, a PSI-blast was performed to determine the most suitable homologous structures. The results indicated that there was no appropriate template structure for homology modeling; therefore, we used a threading method for the HBsAg model's construction. A Phyre2 server was applied to predict the 3D structure of the HBsAg; this server utilizes the alignment of hidden Markov models using an HMM-HMM comparison, which can significantly improve the accuracy of the alignment and detection rates. It also includes a new antibody initio folding simulation called Posing, for multi-template modeling and antibody initio protein structure prediction (24). Finally, a model was generated by Phyre2 and then subsequently refined using the ModRefiner (25). After several energy minimization steps using GROMACS 43a1 force field, the visualization of the refined model as well as the generation of the G145R mutant were performed by PyMOL software (26). To quantitatively evaluate the modeled 3D structure, several web tools, including VADAR, PROSESS (<http://www.prosess.ca/>), and SAVES (nihserver.mbi.ucla.edu/SAVES/), were used simultaneously (27). At the same time, the wild-type and G145R mutant HBsAg proteins were structurally aligned, and their root mean square deviation (RMSD) and template modeling (TM) scores were computed using the SuperPose and TM-align servers, respectively (28, 29).

3.3. Molecular Docking

It is now well established that the monoclonal antibody 12 (MAb12) can selectively bind to the surface antigen of the hepatitis B virus (30). The 3D structure of MAb12 was obtained from the PDB database (<http://www.rcsb.org/pdb>; PDB ID: 4Q0X). Unwanted ligands, ions, and molecules were removed from the PDB file using PyMOL software, and the final refined MAb12 structure was used in molecular docking studies. Molecular docking of the HBsAg and MAb12 structures was performed using the ClusPro web server (31). The binding affinity of the HBsAg-MAb12 complex was calculated according to the coefficient weights as follows:

$$E = 0.20E_{\text{rep}} + -0.40E_{\text{att}} + 600E_{\text{elec}} + 0.25E_{\text{DARS}}$$

Where E_{rep} and E_{att} represent the repulsive and attractive components in the implementation steps of the van der Waals energy, respectively. E_{elec} is the Coulombic electrostatic energy, and E_{DARS} denotes a new class of knowledge-based interaction potentials. See Brenke et al. paper for more details (32).

3.4. Molecular Dynamics (MD) Simulations

MD simulation has been widely used in structural biology investigations and can serve as a powerful tool to determine the atomic-level behavior of biological events, such as protein conformational changes under different physiological conditions (33). MD simulations for both the G145R mutant and the wild-type HBsAg were conducted using GROMACS v5.0.2 package (34). The predicted 3D structures were solvated in a solvation box with 10Å distance between the edges of the box and the protein fragments. Na⁺ and Cl⁻ ions were added to neutralize the system. Then, the equilibrated systems were subjected to a 10-ns MD simulation in the isothermal-isobaric (NPT) ensemble using the leap-frog algorithm with an integration time step of 0.002 ps.

3.5. Evaluation of Protein Antigenicity

It has been sufficiently established that amino acid substitutions in both within and outside of the “a” determinant can cause a reduced binding affinity to monoclonal antibodies (35). To assess the antigenic potential, both wild-type and G145R mutant HBsAg were subjected to the antibody epitope prediction server IEDB-AR (36), which provides multiple tools to predict MHC class I and MHC class II restricted T-cell epitopes as well as linear and discontinuous B-cell epitopes.

4. Results

4.1. G145R Mutation Alters the Secondary Structure and Membrane Orientation of the HBsAg

G145 is located in the second loop of the MHR within the “a” determinant, a flexible coil stabilized by two disulfide bonds that play a key role in the antigenicity of HBsAg. A secondary structure analysis of the G145R mutant revealed that this substitution inserted a new β -strand at the 121 - 124 position (Figure 1). However, the differences between the secondary structure of the G145R mutant and the wild-type HBsAg at all other regions of the protein were extensively subtle.

An analysis of the transmembrane regions revealed that the number of transmembrane helices in the G145R mutant was not altered compared to the wild-type. However, the orientation of transmembrane segments between the G145R mutant and wild-type was clearly different, suggesting the possible impact of the G145R mutation on the altered localization of the mutant HBsAg within the ER membrane. The “a” determinant region in the wild-type and G145R mutants is positioned at the ER lumen and in the cytoplasmic area, respectively (Figure 2). Accordingly, any alteration in the membrane topology of the HBsAg can affect the distribution of this protein.

4.2. Prediction and Evaluation of the 3D Structure of the HBsAg

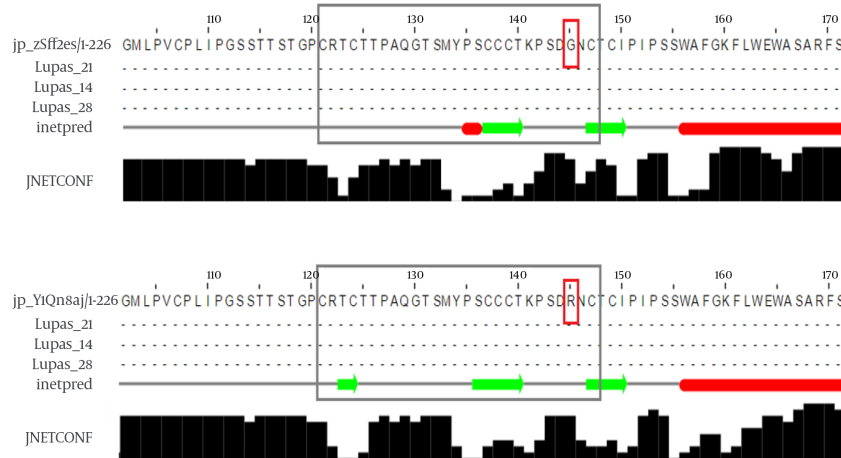
The predicted 3D structure of the HBsAg after the refining and energy minimization steps is indicated in Figure 3. A Ramachandran plot of the final refined HBsAg model obtained from PROCHECK revealed that 87.7%, 9.1%, 1.1%, and 2.1% of the residues were located in the most favored, additionally allowed, generously allowed, and disallowed regions, respectively (Figure 4A). The overall model quality was evaluated using the ProSA Z-score, which calculates the overall quality of the model to determine whether the quality of the input model is positioned within the range of scores typically found for experimentally solved protein structures (37). The ProSA Z-score for the final HBsAg model was -1.39, which falls within the normal range of experimentally validated protein structures (Figure 4B).

Further quality analysis was carried out using the MolProbity score. This score for the modeled 3D structure of the HBsAg was calculated as 1.94, which indicates a good resolution of this model. The MolProbity is derived from a combination of the clash score, rotamer, and Ramachandran evaluations. In addition, the MolProbity clash score was 8.4 (the number of serious steric overlaps (0.4 Å³) per 1000 atoms). Structures with a high quality usually score below 10. 3D verification was allocated to determine the compatibility of the HBsAg 3D model with its own amino acid sequences. The results indicated that 69.47% of the residues were scored 0.2. The outcome is considered acceptable when more than 65% of the residues are 0.2. The predicted structure was further validated using ERRAT, which analyzes the statistics of non-bonded interactions between different atom types. A higher ERRAT value suggests a higher quality 3D model. The ERRAT score for the HBsAg model was 76.09%, which was satisfactory; this finding was also in agreement with previous overall quality scores.

4.3. The Effect of G145R Substitution on the 3D Structure of the HBsAg

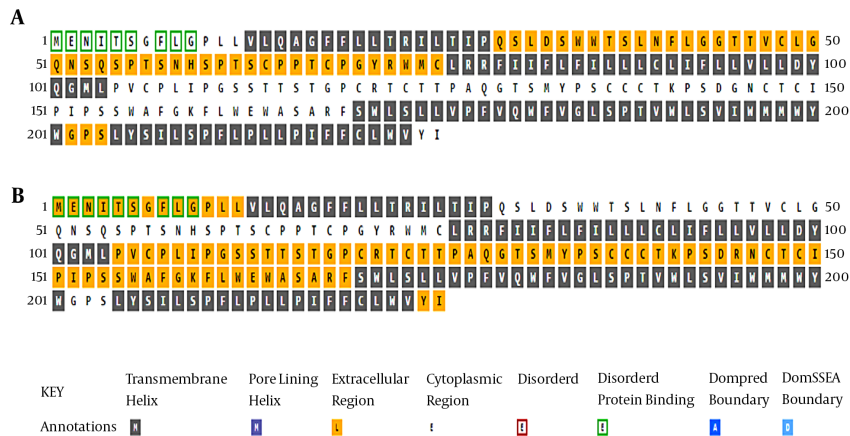
Although the superposition of two structures demonstrates an inconsiderable alteration in the overall 3D structure, this mutation can induce local changes in the structure of the protein, particularly in the “a” determinant region. Figure 5A represents the structural alignment of the G145R mutant and wild-type HBsAg. Some of these changes, such as the number of residues with an H-bond, the total accessible surface area, and the total volume, were computed using the VADAR web server. Compared to the G145 residue, the R145 can interfere with the integrity of the HBsAg antigenic loop by forming an H-bond with C147, a key residue involved in the formation of the second antigenic loop of the HBsAg (Figure 5B). The very low RMSD

Figure 1. The Effect of G145R Substitution on the Secondary Structure of the Wild-Type (Up) and G145R (Down) Mutations



Extended β -strands and α -helices are shown in green and red colors, respectively. The “a” determinant region and mutation position are shown in gray and red boxes, respectively.

Figure 2. Transmembrane Analysis of the A, Wild-Type and B, G145R Mutant HBsAg



Key annotations are shown at the bottom of the figure. Please note that the annotations are for the cell membrane; the extracellular and cytoplasmic regions refer to the cytosolic and lumen sides of the ER, respectively.

value (0.38) and the high TM-score (0.99) that resulted from the structural alignment demonstrate that the G145R mutant and wild-type HBsAg have almost the same folding character.

4.4. G145R Mutation Decreases the Binding Affinity of the HBsAg to the MAb12

Molecular docking showed that the G145R mutation caused a noticeable decreased binding affinity between the HBsAg and MAb12. The wild-type and G145R mutant HBsAgs were bound to the MAb12 with weighted scores of -

626.7 and -309.1, respectively, implicating the lower binding affinity of G145R mutant to MAb12 compared to wild type. The HBsAg-MAb12 complexes were visualized using the DIMPLOT module of the LigPlot+ package to determine their polar bonds and non-polar connections (38). The results demonstrated that the G145R mutation likely reduced the number of H-bonds through residue-residue approximation constraints with adjacent amino acids. Furthermore, a DIMPLOT analysis indicated that G145 and N146 were actively involved in the HBsAg-MAb12 interaction. In the mutant HBsAg, R145 did not form any H-bond with

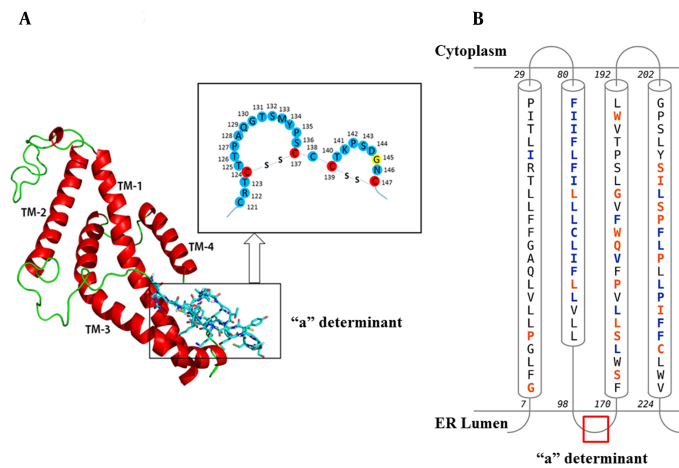
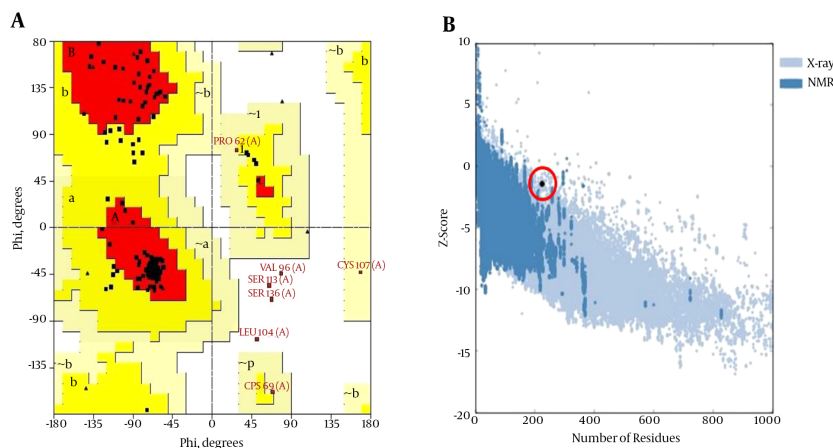


Figure 3. A) The Predicted 3D Structure of the HBsAg Along with a Schematic Representation of the “a” Determinant Region. Transmembrane helices (TM1-4) are shown in red and the mutation site (amino acid 145) is yellow; B, Topology of HBsAg helices within the ER Membrane. Contact Colorcodes: Orange and Blue Letters Refer to Helix Contact and Membrane Contact, Respectively.

Figure 4. A, A Ramachandran Plot Generated by PROCHECK and B, the ProSA Z-Score for the HBsAg Model (Open Red Circle)



The residues in the most favored (red), additionally allowed (yellow), generously allowed (pale yellow), and disallowed regions (white) of the Ramachandran plot are indicated. The structures determined by different methods (X-ray, NMR) are distinguished by different colors in the ProSA Z-score plot.

MAb12. The larger size of the R145 side chain seems to be involved in the inhibition of H-bond formation between the N146 and MAb12 residues (Figure 6). More details regarding the molecular docking results are shown in Table 1.

4.5. G145R Mutation Reduces the Antigenic Potential of the HBsAg

An evaluation of the protein antigenicity revealed that the antigenic potential of G145R mutant HBsAg was reduced compared to the wild-type (Figure 7). The antigenicity scores for the G145 and R145 residues were calculated as

1.19 and 0.9, respectively, implicating a key role for G145 in the antigenic potential of the HBsAg.

4.6. MD Simulations

RMSD is a reliable value that is widely used for evaluating the structural differences between proteins and is also considered to be an indicator of structural stability. The RMSD plots of the wild-type and G145R mutant HBsAg revealed that the G145R mutation further stabilized the HBsAg’s structure (Figure 8A). We also calculated the radius of gyration (Rg) values for both HBsAg types (Figure 8B). The

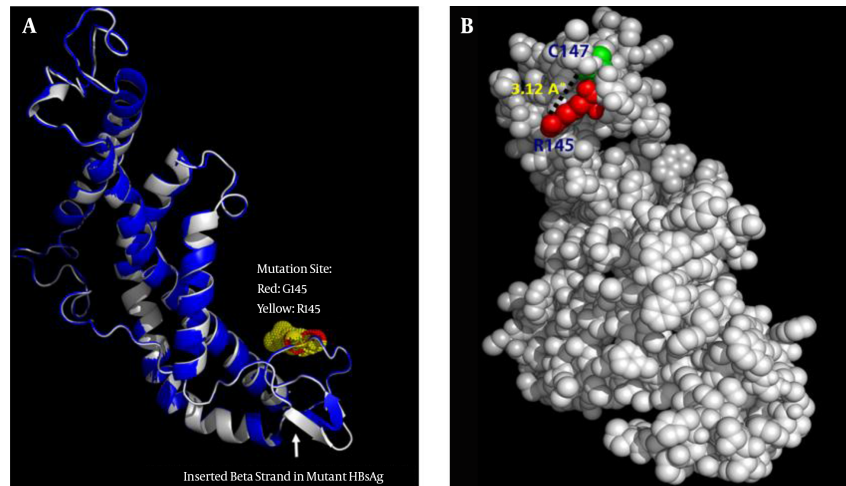
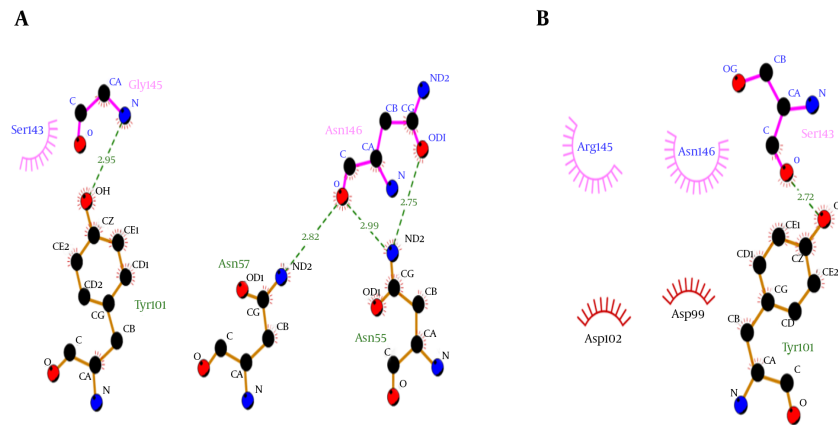


Figure 5. A, Superposition of the wild-type HBsAg (blue) and the G145R mutant (gray). The arrow indicates the position of the inserted β -strand in the mutant HBsAg's "a" determinant region. B, Representative positioning of the H-bond between the R145 and C147 mutation in the 3D structure of the G145R mutant HBsAg.

Figure 6. Representation of the A, Wild and B, G145R Mutant HBsAg-MAb12 Interaction



H-bonds are shown with dotted lines. Unbound residues indicate non-polar connections.

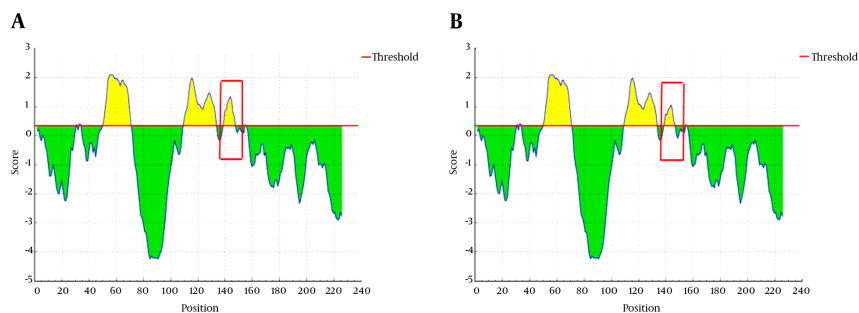
Table 1. Binding Energies of the Wild and Mutant HBsAg in Complex with MAb12

HBsAg type	MAb12			
	Center Energy	Lowest Energy	Cluster No. ^a	"a" Determinant H-Bond No.
Wild-type HBsAg	-601.8	-626.7	177	14
G145R mutant HBsAg	-290.9	-309.1	66	10

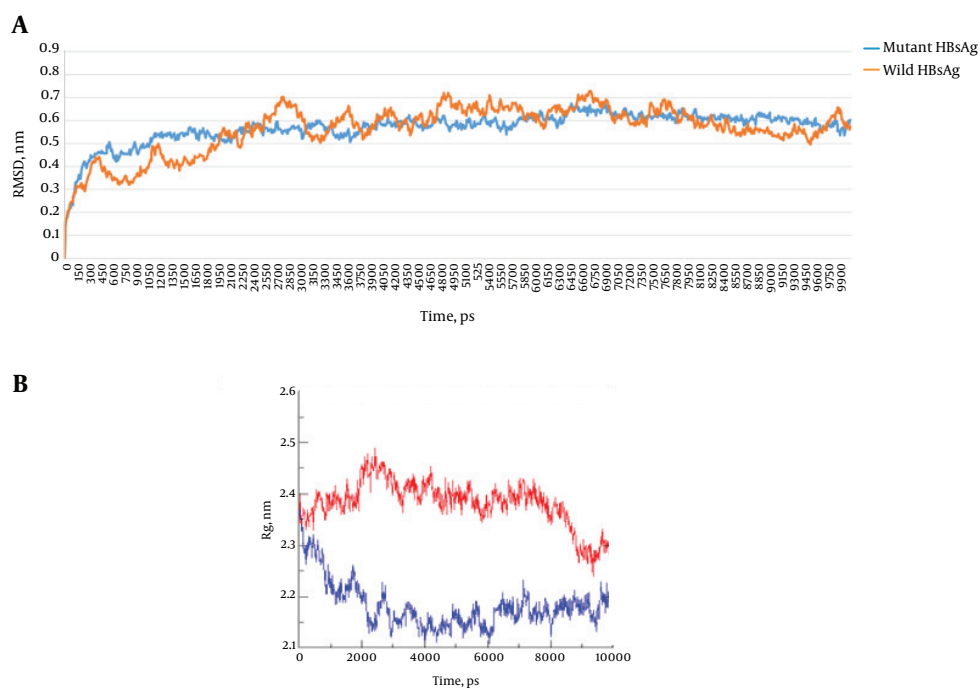
^aThe cluster with the largest number of low-energy structures typically contains the native fold.

Rg is most often used in the determination of protein compactness (39). A comparison of the Rg plots demonstrated a higher compactness of the mutant HBsAg compared to the wild-type HBsAg.

To determine the structural dynamics of the wild-type and G145R mutant, the root mean square fluctuation (RMSF) of the $C\alpha$ of the HBsAg protein was compared between the trajectories generated at 300 K to gain an in-

Figure 7. Analysis of HBsAg Antigenicity in the A, Wild-type and B, G145R Mutant Proteins

The antigenic and non-antigenic segments are shown in yellow and green, respectively.

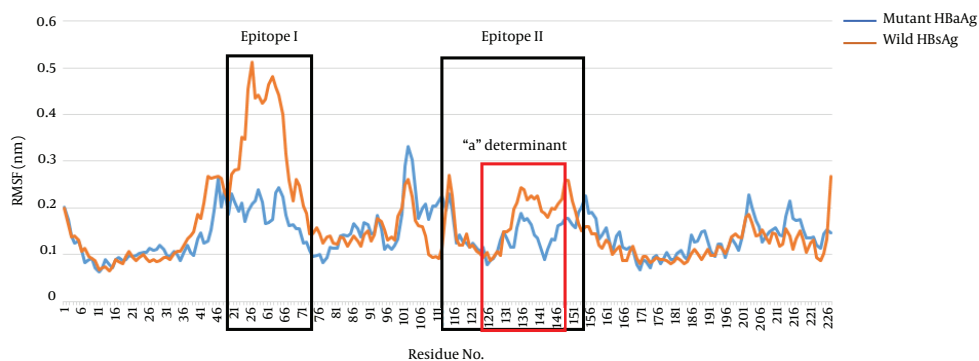
Figure 8. A, RMSD and **B,** Rg Plots of the G145R Mutant and Wild-Type HBsAg

The Rg plots of the wild- and mutant types are shown in red and blue, respectively.

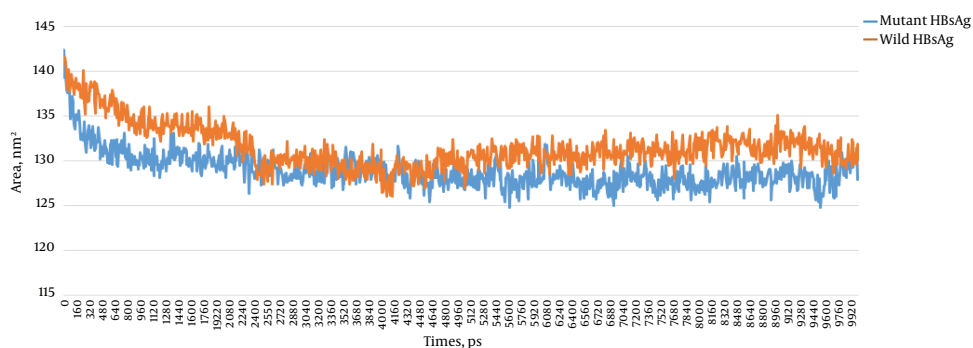
sight into the flexible nature of the G145R mutant compared with the wild-type. Interestingly, the flexibility of the mutant HBsAg, especially in the antigenic regions, was considerably reduced, indicating that the G145R mutation resulted in increased protein rigidity (Figure 9), which makes the HBsAg unsuitable for interacting with antibodies.

A calculation of the accessibility surface area (ASA) showed that the surface accessibility of the G145R mutant HBsAg was reduced upon G145R substitution. ASA plots of

the wild-type and mutant HBsAg are shown in Figure 10. A decrease in the mutant HBsAg ASA suggests that the G145R mutation converts the HBsAg structure to a compact configuration with buried functional segments, such as epitopes. The ASA of the side chains in the wild-type and the G145R mutant were 13,219.2 and 13,017.8 Å², respectively.

Figure 9. RMSF Plots of Wild- and G145R Mutant Types after 10-ns MD Simulations

Predicted epitopes are shown in black boxes. The "a" determinant region is in a red box.

**Figure 10.** ASA Plots of the G145R Mutant and Wild-Type HBsAg after 10-ns MD Simulations

5. Discussion

A variety of HBsAg mutations has been reported within the "a" determinant region (4). Of these, G145R is the commonest and the most widely studied HBV immune escape mutation, emerging naturally or in response to vaccination or hepatitis B immunoglobulin (HBIG) therapy. Previous studies have indicated that the ability to neutralize anti-HBs against this variant could be diminished (40-42). In the current study, we investigated the 3D structure and molecular dynamics of the HBsAg at position 145 for both the wild-type and the mutant. Amino acid mutations within the critical positions of structural proteins may influence its stability and conformation and also affect its properties and interactions with other proteins. Several studies have indicated that the 3D structures of proteins play a pivotal role in their biological activity and interactions with other molecules (43).

In this study, we found that the secondary structure of the G145R HBsAg was significantly affected, with a gain of a β -strand as well as the loss of α -helix contents. It is now

widely accepted that β -strands play a key role in the aggregation of proteins. The aggregates have more β -strand structures and less α -helix content (44). Taken together, the G145R mutation can increase the rigidity and aggregation potential of HBsAg's "a" determinant, which alters its immunogenic activity and secretion. Recent studies have shown that the antigenic determinants of the HBsAg are highly conformation-dependent; therefore, any alteration in the "a" determinate region can reduce or inactivate the antigenic activity of this antigen (45).

Moreover, our results demonstrated that the G145R mutation was highly capable of increasing the compactness of the HBsAg. The compactness of a protein is generally described as the ratio of the ASA of a protein to the surface area of the ideal sphere of the same volume (39). These results confirmed the relationship between protein compactness and surface accessibility. Indeed, we found that the G145R mutation reduced the ASA of the HBsAg by increasing the protein's compactness and rigidity. An increase in protein compactness is one explanation for the

increased protein rigidity that leads to enhanced protein stability (46). It is plausible that a reduced protein ASA also may elevate the protein's stability (47). Furthermore, an analysis of Rg demonstrated that the atoms of the G145R mutant were highly packed within the protein structure, resulting in increased protein stability. In contrast with the wild-type HBsAg, the RMSD of the coordinates of all C α atoms in the G145R mutant demonstrated that the HBsAg mutant remained very stable and folded over the course of 10 ns at 300 K. The RMSD and Rg values are highly reliable measures for determining a protein's compactness and stability under physiological conditions (48, 49). There is also a correlation between the C α RMSF measures and protein flexibility; therefore, proteins with higher RMSF values are generally considered to have more flexible regions (50). The present study showed that the average C α RMSF of the G145R mutant was clearly lower than that of the wild-type, especially in the antigenic regions. This finding may be an important factor involved in the antibody escape of HBsAg that contain the G145R mutation (51).

An antigenic potential analysis of the wild-type HBsAg and the G145R mutant revealed a significant decrease of antigenicity in the mutant type. This finding was supported by other results from molecular dynamic and docking studies. The lower binding affinity between G145R and MAb12 compared with the wild-type protein indicated the intrinsic potential of this mutant to escape HBsAg neutralization using specific antibodies, as reported in previous studies (52-54). According to the detailed figures of amino acid interactions revealed by DIMPLOT, the substitution of Gly with Arg leads to a reduction in the total number of H-bonds between the HBsAg and its monoclonal antibody. Protein-protein docking results showed that unlike G145, R145 was not able to form an H-bond with MAb12. Additionally, it prevents the appropriate interaction of N146 with its target residues in MAb12. Therefore, R145 may change the arrangement of the H-bond network in the antigenic loops of the G145R mutant HBsAg. Moreover, when G145 is replaced by R145, a new H-bond forms between this residue and C147, which may also alter the spatial conformation of the second loop of the "a" determinant region.

Molecular dynamic analysis revealed a significant increase in the compactness of the mutant protein as well as a decrease in the flexibility of the antigenic loops and the total accessible surface area of the mutant type. All these results indicate that the antigenic loops in the G145R mutant are not as exposed as those in the wild-type HBsAg, and it can reduce its availability to specific HBsAg antibodies, which may explain the lower immunogenic potential of the G145R mutant protein. Reduced immunogenicity in "a" determinant mutants, especially the G145R mutant, has been observed in previous studies (13, 55). These mu-

tations can specifically change the binding affinity to antibody as well as the sensitivity of diagnostic tests. Glycine is an amino acid with a non-polar side chain, while Arginine has a polar, charged (at physiological pH), and highly bulky side chain. Thus, differences in the physicochemical properties of these residues may affect the 3D conformation and therefore the steric hindrance between other residues (56).

The G145R mutation is an immune escape mutation that causes problems with diagnostic assays and a poor response to vaccines. Mutants can replicate, even in vaccinated individuals, so current vaccines are often ineffective in the production of suitable antibodies (54, 57, 58). Therefore, these mutants and their subsequent alterations in the HBsAg structure and characteristics deserve significant attention to facilitate the design of more specific antibodies for vaccines and serology designations.

In conclusion, this study provides some *in silico* evidence about the impacts of the G145R mutation on the structure and immunogenic activity of the HBsAg. Our analyses revealed that the G145R mutation induces a local change in the "a" determinant conformation. The results suggest that the HBsAg can escape from the host's immune system, vaccine, and HBIG as well as from diagnostic assays due to a local change in the "a" determinant region. However, the results need to be validated experimentally.

Acknowledgments

This study was supported by Tehran University of Medical Sciences.

Footnotes

Authors' Contribution: Reza Rezaee: literature search, writing, and reviewing; Vahdat Poortahmasebi: study concept, design, and drafting of the manuscript; Mansour Poorebrahim and Solmaz Sadeghi: writing, bioinformatics analysis, and revision of the manuscript; Saeideh Najafi and Alieh Pourdash: interpretation of the data and language revision of the manuscript; Seyed Moayed Alavian and Seyed Ehsan Alavian contributed equally to this article.

Financial Disclosure: None declared.

Funding/Support: The authors did not receive financial support for this article.

References

1. Tiollais P, Pourcel C, Dejean A. The hepatitis B virus. *Nature*. 1985;317(6037):489-95. [PubMed: 2995835].

2. Chen P, Gan Y, Han N, Fang W, Li J, Zhao F, et al. Computational evolutionary analysis of the overlapped surface (S) and polymerase (P) region in hepatitis B virus indicates the spacer domain in P is crucial for survival. *PLoS One*. 2013;**8**(4):60098. doi: [10.1371/journal.pone.0060098](https://doi.org/10.1371/journal.pone.0060098). [PubMed: [23577084](https://pubmed.ncbi.nlm.nih.gov/23577084/)].
3. Ashton-Rickardt PG, Murray K. Mutations that change the immunological subtype of hepatitis B virus surface antigen and distinguish between antigenic and immunogenic determination. *J Med Virol*. 1989;**29**(3):204-14. [PubMed: [2693611](https://pubmed.ncbi.nlm.nih.gov/2693611/)].
4. Alavian SM, Carman WF, Jazayeri SM. HBsAg variants: diagnostic-escape and diagnostic dilemma. *J Clin Virol*. 2013;**57**(3):201-8. doi: [10.1016/j.jcv.2012.04.027](https://doi.org/10.1016/j.jcv.2012.04.027). [PubMed: [22789139](https://pubmed.ncbi.nlm.nih.gov/22789139/)].
5. Weber B. Diagnostic impact of the genetic variability of the hepatitis B virus surface antigen gene. *J Med Virol*. 2006;**78** Suppl 1:S59-65. doi: [10.1002/jmv.20610](https://doi.org/10.1002/jmv.20610). [PubMed: [16622880](https://pubmed.ncbi.nlm.nih.gov/16622880/)].
6. Weber B, Melchior W, Gehrke R, Doerr HW, Berger A, Rabenau H. Hepatitis B virus markers in anti-HBc only positive individuals. *J Med Virol*. 2001;**64**(3):312-9. [PubMed: [11424120](https://pubmed.ncbi.nlm.nih.gov/11424120/)].
7. El Chaar M, Candotti D, Crowther RA, Allain JP. Impact of hepatitis B virus surface protein mutations on the diagnosis of occult hepatitis B virus infection. *Hepatology*. 2010;**52**(5):1600-10. doi: [10.1002/hep.23886](https://doi.org/10.1002/hep.23886). [PubMed: [20815025](https://pubmed.ncbi.nlm.nih.gov/20815025/)].
8. Besharat S, Katoonzadeh A, Moradi A. Potential mutations associated with occult hepatitis B virus status. *Hepat Mon*. 2014;**14**(5):15275. doi: [10.5812/hepatmon.15275](https://doi.org/10.5812/hepatmon.15275). [PubMed: [24829588](https://pubmed.ncbi.nlm.nih.gov/24829588/)].
9. Shahmoradi S, Yahyapour Y, Mahmoodi M, Alavian SM, Fazeli Z, Jazayeri SM. High prevalence of occult hepatitis B virus infection in children born to HBsAg-positive mothers despite prophylaxis with hepatitis B vaccination and HBIG. *J Hepatol*. 2012;**57**(3):515-21. doi: [10.1016/j.jhep.2012.04.021](https://doi.org/10.1016/j.jhep.2012.04.021). [PubMed: [22617152](https://pubmed.ncbi.nlm.nih.gov/22617152/)].
10. Purdy MA. Hepatitis B virus S gene escape mutants. *Asian J Transfus Sci*. 2007;**1**(2):62-70. doi: [10.4103/0973-6247.33445](https://doi.org/10.4103/0973-6247.33445). [PubMed: [21938236](https://pubmed.ncbi.nlm.nih.gov/21938236/)].
11. Bock CT, Tillmann HL, Torresi J, Klemmner J, Locarnini S, Manns MP, et al. Selection of hepatitis B virus polymerase mutants with enhanced replication by lamivudine treatment after liver transplantation. *Gastroenterology*. 2002;**122**(2):264-73. [PubMed: [11832441](https://pubmed.ncbi.nlm.nih.gov/11832441/)].
12. Norouzi M, Ramezani F, Khehive A, Karimzadeh H, Alavian SM, Malekzadeh R, et al. Hepatitis B Virus Genotype D is the Only Genotype Circulating in Iranian Chronic Carriers, the Unique Pattern of Genotypic Homogeneity. *J Gastroenterol Hepatol Res*. 2014;**3**(9):1238-43. doi: [10.17554/j.issn.2224-3992.2014.03.418](https://doi.org/10.17554/j.issn.2224-3992.2014.03.418).
13. Ma Q, Wang Y. Comprehensive analysis of the prevalence of hepatitis B virus escape mutations in the major hydrophilic region of surface antigen. *J Med Virol*. 2012;**84**(2):198-206. doi: [10.1002/jmv.23183](https://doi.org/10.1002/jmv.23183). [PubMed: [22170538](https://pubmed.ncbi.nlm.nih.gov/22170538/)].
14. Ireland JH, O'Donnell B, Basuni AA, Kean JD, Wallace LA, Lau GK, et al. Reactivity of 13 in vitro expressed hepatitis B surface antigen variants in 7 commercial diagnostic assays. *Hepatology*. 2000;**31**(5):1176-82. doi: [10.1053/he.2000.6407](https://doi.org/10.1053/he.2000.6407). [PubMed: [10796895](https://pubmed.ncbi.nlm.nih.gov/10796895/)].
15. Folgori A, Tafi R, Meola A, Felici F, Galfre G, Cortese R, et al. A general strategy to identify mimotopes of pathological antigens using only random peptide libraries and human sera. *EMBO J*. 1994;**13**(9):2236-43. [PubMed: [7514533](https://pubmed.ncbi.nlm.nih.gov/7514533/)].
16. Motti C, Nuzzo M, Meola A, Galfre G, Felici F, Cortese R, et al. Recognition by human sera and immunogenicity of HBsAg mimotopes selected from an M13 phage display library. *Gene*. 1994;**146**(2):191-8. [PubMed: [8076818](https://pubmed.ncbi.nlm.nih.gov/8076818/)].
17. Chen YC, Delbrook K, Dealwis C, Mimms L, Mushahwar IK, Mandeck W. Discontinuous epitopes of hepatitis B surface antigen derived from a filamentous phage peptide library. *Proc Natl Acad Sci U S A*. 1996;**93**(5):1997-2001. [PubMed: [8700874](https://pubmed.ncbi.nlm.nih.gov/8700874/)].
18. Stirk HJ, Thornton JM, Howard CR. A topological model for hepatitis B surface antigen. *Intervirology*. 1992;**33**(3):148-58. [PubMed: [1500275](https://pubmed.ncbi.nlm.nih.gov/1500275/)].
19. Westbrook J, Feng Z, Chen L, Yang H, Berman HM. The Protein Data Bank and structural genomics. *Nucleic Acids Res*. 2003;**31**(1):489-91. [PubMed: [12520059](https://pubmed.ncbi.nlm.nih.gov/12520059/)].
20. Drozdetskiy A, Cole C, Procter J, Barton GJ. JPred4: a protein secondary structure prediction server. *Nucleic Acids Res*. 2015;**43**(W1):W389-94. doi: [10.1093/nar/gkv332](https://doi.org/10.1093/nar/gkv332). [PubMed: [25883141](https://pubmed.ncbi.nlm.nih.gov/25883141/)].
21. Rost B, Sander C, Schneider R. PHD-an automatic mail server for protein secondary structure prediction. *Bioinformatics*. 1994;**10**(1):53-60. doi: [10.1093/bioinformatics/10.1.53](https://doi.org/10.1093/bioinformatics/10.1.53).
22. McGuffin LJ, Bryson K, Jones DT. The PSIPRED protein structure prediction server. *Bioinformatics*. 2000;**16**(4):404-5. [PubMed: [10869041](https://pubmed.ncbi.nlm.nih.gov/10869041/)].
23. Jones DT, Taylor WR, Thornton JM. A model recognition approach to the prediction of all-helical membrane protein structure and topology. *Biochemistry*. 1994;**33**(10):3038-49. [PubMed: [8130217](https://pubmed.ncbi.nlm.nih.gov/8130217/)].
24. Kelley LA, Mezulis S, Yates CM, Wass MN, Sternberg MJ. The Phyre2 web portal for protein modeling, prediction and analysis. *Nat Protoc*. 2015;**10**(6):845-58. doi: [10.1038/nprot.2015.053](https://doi.org/10.1038/nprot.2015.053). [PubMed: [25950237](https://pubmed.ncbi.nlm.nih.gov/25950237/)].
25. Xu D, Zhang Y. Improving the physical realism and structural accuracy of protein models by a two-step atomic-level energy minimization. *Biophys J*. 2011;**101**(10):2525-34. doi: [10.1016/j.bpj.2011.10.024](https://doi.org/10.1016/j.bpj.2011.10.024). [PubMed: [22098752](https://pubmed.ncbi.nlm.nih.gov/22098752/)].
26. DeLano WL. The PyMOL molecular graphics system. ; 2002.
27. Willard L, Ranjan A, Zhang H, Monzavi H, Boyko RF, Sykes BD, et al. VADAR: a web server for quantitative evaluation of protein structure quality. *Nucleic Acids Res*. 2003;**31**(13):3316-9. [PubMed: [12824316](https://pubmed.ncbi.nlm.nih.gov/12824316/)].
28. Maiti R, Van Domselaar GH, Zhang H, Wishart DS. SuperPose: a simple server for sophisticated structural superposition. *Nucleic Acids Res*. 2004;**32**(Web Server issue):590-4. doi: [10.1093/nar/gkh477](https://doi.org/10.1093/nar/gkh477). [PubMed: [15215457](https://pubmed.ncbi.nlm.nih.gov/15215457/)].
29. Zhang Y, Skolnick J. TM-align: a protein structure alignment algorithm based on the TM-score. *Nucleic Acids Res*. 2005;**33**(7):2302-9. doi: [10.1093/nar/gki524](https://doi.org/10.1093/nar/gki524). [PubMed: [15849316](https://pubmed.ncbi.nlm.nih.gov/15849316/)].
30. Appel JR, Muller S, Benkirane N, Houghten RA, Pinilla C. Highly specific, cross-reactive sequences recognized by an anti-HBsAg antibody identified from a positional scanning synthetic combinatorial library. *Pept Res*. 1996;**9**(4):174-82. [PubMed: [8914164](https://pubmed.ncbi.nlm.nih.gov/8914164/)].
31. Comeau SR, Gatchell DW, Vajda S, Camacho CJ. ClusPro: an automated docking and discrimination method for the prediction of protein complexes. *Bioinformatics*. 2004;**20**(1):45-50. [PubMed: [14693807](https://pubmed.ncbi.nlm.nih.gov/14693807/)].
32. Brenke R, Hall DR, Chuang GY, Comeau SR, Bohnuud T, Beglov D, et al. Application of asymmetric statistical potentials to antibody-protein docking. *Bioinformatics*. 2012;**28**(20):2608-14. doi: [10.1093/bioinformatics/bts493](https://doi.org/10.1093/bioinformatics/bts493). [PubMed: [23053206](https://pubmed.ncbi.nlm.nih.gov/23053206/)].
33. Klepeis JL, Lindorff-Larsen K, Dror RO, Shaw DE. Long-timescale molecular dynamics simulations of protein structure and function. *Curr Opin Struct Biol*. 2009;**19**(2):120-7. doi: [10.1016/j.sbi.2009.03.004](https://doi.org/10.1016/j.sbi.2009.03.004). [PubMed: [19361980](https://pubmed.ncbi.nlm.nih.gov/19361980/)].
34. Pronk S, Pall S, Schulz R, Larsson P, Bjelkmar P, Apostolov R, et al. GROMACS 4.5: a high-throughput and highly parallel open source molecular simulation toolkit. *Bioinformatics*. 2013;**29**(7):845-54. doi: [10.1093/bioinformatics/btt055](https://doi.org/10.1093/bioinformatics/btt055). [PubMed: [23407358](https://pubmed.ncbi.nlm.nih.gov/23407358/)].
35. Dindoost P, Jazayeri SM, Karimzadeh H, Saberfar E, Miri SM, Alavian SM. HBsAg Variants: Common Escape Issues. *Jundishapur J Microb*. 2012;**5**(4):521-7. doi: [10.5812/jjm.4243](https://doi.org/10.5812/jjm.4243).
36. Zhang Q, Wang P, Kim Y, Haste-Andersen P, Beaver J, Bourne PE, et al. Immune epitope database analysis resource (IEDB-AR). *Nucleic Acids Res*. 2008;**36**(Web Server issue):513-8. doi: [10.1093/nar/gkn254](https://doi.org/10.1093/nar/gkn254). [PubMed: [18515843](https://pubmed.ncbi.nlm.nih.gov/18515843/)].
37. Wiederstein M, Sippl MJ. ProSA-web: interactive web service for the recognition of errors in three-dimensional structures of proteins. *Nucleic Acids Res*. 2007;**35**(Web Server issue):407-10. doi: [10.1093/nar/gkm290](https://doi.org/10.1093/nar/gkm290). [PubMed: [17517781](https://pubmed.ncbi.nlm.nih.gov/17517781/)].
38. Laskowski RA, Swindells MB. LigPlot+: multiple ligand-protein interaction diagrams for drug discovery. *J Chem Inf Model*. 2011;**51**(10):2778-86. doi: [10.1021/ci200227u](https://doi.org/10.1021/ci200227u). [PubMed: [21919503](https://pubmed.ncbi.nlm.nih.gov/21919503/)].
39. Lobanov M, Bogatyreva NS, Galzitskaia OV. Radius of gyration is indicator of Radius of protein structure compactness. *Mol Biol*. 2008;**42**(4):701-6. [PubMed: [18856071](https://pubmed.ncbi.nlm.nih.gov/18856071/)].

40. Sheldon J, Soriano V. Hepatitis B virus escape mutants induced by antiviral therapy. *J Antimicrob Chemother.* 2008;**61**(4):766-8. doi: [10.1093/jac/dkn014](https://doi.org/10.1093/jac/dkn014). [PubMed: [18218641](https://pubmed.ncbi.nlm.nih.gov/18218641/)].
41. Locarnini SA, Yuen L. Molecular genesis of drug-resistant and vaccine-escape HBV mutants. *Antivir Ther.* 2010;**15**(3 Pt B):451-61. doi: [10.3851/IMP1499](https://doi.org/10.3851/IMP1499). [PubMed: [20516565](https://pubmed.ncbi.nlm.nih.gov/20516565/)].
42. Ishigami M, Honda T, Ishizu Y, Onishi Y, Kamei H, Hayashi K, et al. Frequent incidence of escape mutants after successful hepatitis B vaccine response and stopping of nucleos(t)ide analogues in liver transplant recipients. *Liver Transpl.* 2014;**20**(10):1211-20. doi: [10.1002/lt.23935](https://doi.org/10.1002/lt.23935). [PubMed: [24961506](https://pubmed.ncbi.nlm.nih.gov/24961506/)].
43. Ponsel D, Bruss V. Mapping of amino acid side chains on the surface of hepatitis B virus capsids required for envelopment and virion formation. *J Virol.* 2003;**77**(1):416-22. [PubMed: [12477846](https://pubmed.ncbi.nlm.nih.gov/12477846/)].
44. Carrotta R, Bauer R, Waninge R, Rischel C. Conformational characterization of oligomeric intermediates and aggregates in beta-lactoglobulin heat aggregation. *Protein Sci.* 2001;**10**(7):1312-8. doi: [10.1110/ps.42501](https://doi.org/10.1110/ps.42501). [PubMed: [11420433](https://pubmed.ncbi.nlm.nih.gov/11420433/)].
45. Gomez-Gutierrez J, Rodriguez-Crespo I, Gonzalez-Ros JM, Ferragut JA, Paul DA, Peterson DL, et al. Thermal stability of hepatitis B surface antigen S proteins. *Biochim Biophys Acta.* 1992;**1119**(3):225-31. [PubMed: [1372181](https://pubmed.ncbi.nlm.nih.gov/1372181/)].
46. Chen J, Lu Z, Sakon J, Stites WE. Increasing the thermostability of staphylococcal nuclease: implications for the origin of protein thermostability. *J Mol Biol.* 2000;**303**(2):125-30. doi: [10.1006/jmbi.2000.4140](https://doi.org/10.1006/jmbi.2000.4140). [PubMed: [11023780](https://pubmed.ncbi.nlm.nih.gov/11023780/)].
47. Hennig M, Darimont B, Sterner R, Kirschner K, Jansonius JN. 2.0 A structure of indole-3-glycerol phosphate synthase from the hyperthermophile *Sulfolobus solfataricus*: possible determinants of protein stability. *Structure.* 1995;**3**(12):1295-306. [PubMed: [8747456](https://pubmed.ncbi.nlm.nih.gov/8747456/)].
48. Maiorov VN, Crippen GM. Significance of root-mean-square deviation in comparing three-dimensional structures of globular proteins. *J Mol Biol.* 1994;**235**(2):625-34. doi: [10.1006/jmbi.1994.1017](https://doi.org/10.1006/jmbi.1994.1017). [PubMed: [8289285](https://pubmed.ncbi.nlm.nih.gov/8289285/)].
49. Tsai CJ, Nussinov R. Hydrophobic folding units at protein-protein interfaces: implications to protein folding and to protein-protein association. *Protein Sci.* 1997;**6**(7):1426-37. doi: [10.1002/pro.5560060707](https://doi.org/10.1002/pro.5560060707). [PubMed: [9232644](https://pubmed.ncbi.nlm.nih.gov/9232644/)].
50. Benson NC, Daggett V. Dymeomics: large-scale assessment of native protein flexibility. *Protein Sci.* 2008;**17**(12):2038-50. doi: [10.1110/ps.037473.108](https://doi.org/10.1110/ps.037473.108). [PubMed: [18796694](https://pubmed.ncbi.nlm.nih.gov/18796694/)].
51. Yu DM, Li XH, Mom V, Lu ZH, Liao XW, Han Y, et al. N-glycosylation mutations within hepatitis B virus surface major hydrophilic region contribute mostly to immune escape. *J Hepatol.* 2014;**60**(3):515-22. doi: [10.1016/j.jhep.2013.11.004](https://doi.org/10.1016/j.jhep.2013.11.004). [PubMed: [24239777](https://pubmed.ncbi.nlm.nih.gov/24239777/)].
52. Chiou HL, Lee TS, Kuo J, Mau YC, Ho MS. Altered antigenicity of 'a' determinant variants of hepatitis B virus. *J Gen Virol.* 1997;**78** (Pt 10):2639-45. doi: [10.1099/0022-1317-78-10-2639](https://doi.org/10.1099/0022-1317-78-10-2639). [PubMed: [9349486](https://pubmed.ncbi.nlm.nih.gov/9349486/)].
53. Cooreman MP, van Roosmalen MH, te Morsche R, Sunnen CM, de Ven EM, Jansen JB, et al. Characterization of the reactivity pattern of murine monoclonal antibodies against wild-type hepatitis B surface antigen to G145R and other naturally occurring "a" loop escape mutations. *Hepatology.* 1999;**30**(5):1287-92. doi: [10.1002/hep.510300508](https://doi.org/10.1002/hep.510300508). [PubMed: [10534351](https://pubmed.ncbi.nlm.nih.gov/10534351/)].
54. Zheng X, Weinberger KM, Gehrke R, Isogawa M, Hilken G, Kemper T, et al. Mutant hepatitis B virus surface antigens (HBsAg) are immunogenic but may have a changed specificity. *Virology.* 2004;**329**(2):454-64. doi: [10.1016/j.virol.2004.08.033](https://doi.org/10.1016/j.virol.2004.08.033). [PubMed: [15518823](https://pubmed.ncbi.nlm.nih.gov/15518823/)].
55. Hou J, Wang Z, Cheng J, Lin Y, Lau GK, Sun J, et al. Prevalence of naturally occurring surface gene variants of hepatitis B virus in non-immunized surface antigen-negative Chinese carriers. *Hepatology.* 2001;**34**(5):1027-34. doi: [10.1053/jhep.2001.28708](https://doi.org/10.1053/jhep.2001.28708). [PubMed: [11679975](https://pubmed.ncbi.nlm.nih.gov/11679975/)].
56. Lehninger AL, Nelson DL, Cox MM. Amino Acids and Peptides. In: Lehninger principles of biochemistry. New York: Worth Publishers; 1993. pp. 111-33.
57. Zhang M, Ge G, Yang Y, Cai X, Fu Q, Cai J, et al. Decreased antigenicity profiles of immune-escaped and drug-resistant hepatitis B surface antigen (HBsAg) double mutants. *Virology.* 2013;**450**:292. doi: [10.1016/j.virol.2013.10.022](https://doi.org/10.1016/j.virol.2013.10.022). [PubMed: [24053482](https://pubmed.ncbi.nlm.nih.gov/24053482/)].
58. Zuckerman JN, Zuckerman AJ. Mutations of the surface protein of hepatitis B virus. *Antiviral Res.* 2003;**60**(2):75-8. [PubMed: [14638401](https://pubmed.ncbi.nlm.nih.gov/14638401/)].